JPE 4-2-7

Electrical Modeling of Renewable Energy Sources and Energy Storage Devices

Sheldon S. Williamson, S. Chowdary Rimmalapudi, and Ali Emadi†

Grainger Power Electronics and Motor Drives Laboratory Electric Power and Power Electronics Center
Illinois Institute of Technology

ABSTRACT

This paper focuses on the electrical modeling techniques of renewable energy sources and storage devices such as batteries, fuel cells (FCs), photovoltaic (PVs) arrays, ultra-capacitors (UCs), and flywheel energy storage systems (FESS). All of these devices are being investigated recently for their typical storage and supply capabilities for various industrial applications. Hence, these devices must be modeled precisely taking into account the concerned practical issues. An obvious advantage of electrically modeling these renewable energy sources and storage devices is the fact that they can easily be simulated in real-time in any CAD simulation program. This paper reviews several types of suitable models for each of the above-mentioned devices and the most appropriate model amongst them is presented. Furthermore, a few important applications of these devices shall also be highlighted.

Keywords : Circuit modeling, Batteries, Fuel cells, Photovoltaic cells, Capacitive energy storage, Flywheels

1. Introduction

Through prior research results, it is well known that energy storage devices provide additional advantages to improve stability, power-quality, and reliability of the power-supply source[1]. The major types of storage devices being considered nowadays include batteries, ultra -capacitors, and flywheel energy systems, which will be presented in this paper. It is empirical that precise storage device models are created and simulated for several applications, such as hybrid electric vehicles (HEV) and various power system applications[2] the performances of batteries, ultra-capacitors, and fly wheel shave, through over the years, been predicted many different mathematical models. Some of the important factors that need to be considered while modeling these energy storage devices include storage capacity, rate of charge/discharge, temperature, and shelf life.

The electrical models of two of the most promising renewable energy sources, namely fuel cells and PV cells, are also described in this paper. They are recently being studied widely as they do not produce much emission and are considered to be environmentally friendly. However, these renewable energy sources are large, complex, and are expensive at the same time. Hence, designing and building new prototypes is a difficult and expensive affair. A suitable solution to overcome this problem is to carry out detailed simulations on accurately modeled devices.

Through this paper, the various types of equivalent electrical models for fuel cells and PV arrays will be

Manuscript received Aug. 5, 2003; revised Mar. 10, 2004.

† Corresponding Author: emadi@iit.edu
Tel : +1/(312) 567-8940; Fax: +1/(312) 567-8976

presented and analyzed for suitability for operation at system levels.

2. Basic Electrical Modeling of Battery Storage Devices

As mentioned earlier, precise battery models are required for several applications such as for the simulation of energy consumption of electric vehicles, portable devices, or for power system applications. The major challenge in modeling a battery source is the non-linear characteristic of the equivalent circuit parameters, which require lengthy experimental and numerical procedures. The battery itself has some internal parameters, which need to be taken care of [1].

In this section, three basic types of battery models shall be presented: ideal model, linear model, and Thevenin model. Lastly, a simple lead-acid battery model for traction applications that can be simulated in the PSpice software will also be presented.

2.1 Ideal Model

The ideal model of a battery basically ignores the internal parameters and, hence, is very simple. Fig. 1(a) depicts an ideal model of a battery wherein it is clear that the model is primarily made up of only a voltage source [1].

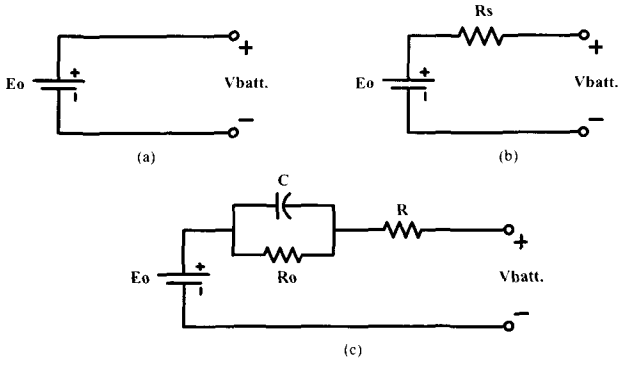

Fig. 1. Battery models: (a) ideal model; (b) linear model; and (c) Thevenin model.

2.2 Linear Model

This is by far the most commonly used battery model. As is clear from Fig. 1(b), this model consists of an ideal battery with open-circuit voltage Eo and an equivalent series resistance Rs [1], [2]. "Vbatt" represents the terminal voltage of the battery. This terminal voltage can be obtained from the open-circuit tests as well as from load tests conducted on a fully charged battery [2].

Although this model is quite widely used, it still does not consider the varying characteristics of the internal impedance of the battery with the varying state of charge (SOC) and electrolyte concentration [2].

2.3 Thevenin Model

This model consists of electrical values of the open-circuit voltage (Eo), internal resistance (R), capacitance (C), and the overvoltage resistance (Ro) [1], [2]. As observed in Fig. 1(c), capacitor C depicts the capacitance of the parallel plates and resistor Ro depicts the non-linear resistance offered by the plate to the electrolyte [2].

In this model, all the elements are assumed to be constants. However, in actuality, they depend on the battery conditions. Thus, this model is also not the most accurate, but is most widely used. In this view, a new approach to evaluate batteries is introduced. The modified model is based on operation over a range of load combinations [3]. The electrical equivalent of the proposed model is depicted in Fig. 2. As is clear from Fig. 2, the main circuit model consists of the following 5 sub-circuits:

(a) E_{batt}: This is a simple DC voltage source designating the voltage in the battery cells.
(b) E_{pol}: It represents the polarization effects due to the availability of active material in the battery.
(c) E_{temp}: It represents the effect of temperature on the battery terminal voltage.
(d) R_{batt}: This is the battery's internal impedance, the value of which depends primarily on the relation between cell voltage and state of charge (SOC) of the battery [3].
(e) V_{sens}: This is basically a voltage source with a value of 0V. It is used to record the value of battery current.

Thus, this simulation model is capable of dealing with various modes of charge/discharge. It is comparatively more precise and can be extended for use with Ni-Cd and Li-ion batteries, which could be applied to hybrid electric

vehicles and other traction applications. Only a few modifications need to be carried out in order to vary the parameters such as load state, current density, and temperature [3].

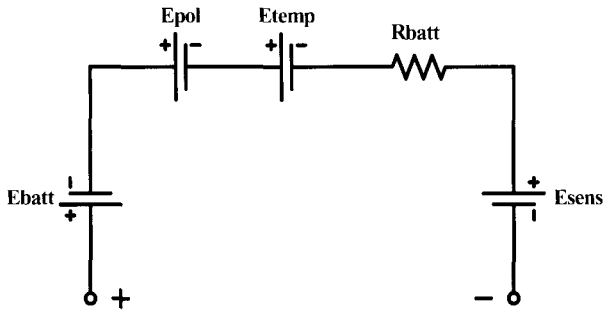

Fig. 2. Main circuit representation of modified battery model.

3. Detailed Electrical Modeling of Renewable Fuel Cell Power Sources

Over the past few years, there have been great environmental concerns shown with respect to emissions from vehicles. These concerns along with the recent developments in fuel cell technology have made room for the hugely anticipated fuel cell market [4]. Fuel Cells are nowadays being considered for applications in hybrid electric vehicles, portable applications, renewable power sources for distributed generation applications, and other similar areas where the emission levels need to be kept to a minimum.

The proton exchange membrane (PEM) fuel cell has the potential of becoming the primary power source for HEVs utilizing fuel cells. However, such fuel cell systems are large and complex and, hence, need accurate models to estimate the auxiliary power systems required for use in the HEV. In this section, the fuel cell modeling techniques will be highlighted, thus, avoiding the need to build huge and expensive prototypes. To have a clearer picture, refer to Fig. 3 showing the schematic representation of a fuel cell/battery hybrid power system.

The battery pack in Fig. 3 is used to compensate for the slow start-up and transient response of the fuel processor [4]. Furthermore, the battery can also be used for the purpose of regenerative braking in the HEV.

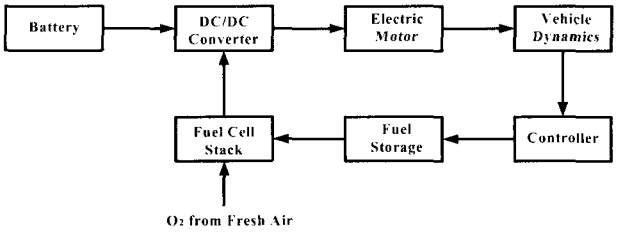

Fig. 3. Schematic representation of a fuel cell/battery hybrid power system.

As mentioned previously, since fuel cell systems are large, complex, and expensive, designing and building new prototypes are difficult [5], [6]. Hence, the feasible alternative is to model the system and examine it through simulations. The fuel cell power system consists of a reformer, a fuel cell stack, and a DC/DC (buck/boost) or DC/AC power converter. The final output from the power electronic converter is in the required DC or AC form acquired from the low-voltage DC output from the fuel cell stack. An electrical equivalent model of a fuel cell power system is discussed here, which can be easily simulated using a computer simulation software.

In the electrical equivalent model, a first-order time-delay circuit with a relatively long time-constant can represent the fuel reformer. Similarly, the fuel cell stack can also be represented by a first-order time-delay circuit, but with a shorter time-constant [5]. Thus, the mathematical model of the reformer and stack are represented as:

$$\frac{Vcr}{Vin} = \frac{\frac{1}{Cr.S}}{Rr + \frac{1}{Cr.S}} = \frac{1}{1 + RrCr.S} \tag{1}$$

$$\frac{Vcs}{Vcr} = \frac{\frac{1}{Cs.S}}{Rs + \frac{1}{Cs.S}} = \frac{1}{1 + RsCs.S} \tag{2}$$

Here, $RrCr = \tau r$ is the time-constant of the reformer and $RsCs = \tau s$ is the time-constant of the fuel cell stack [5]. The equivalent circuit is as shown in Fig. 4.

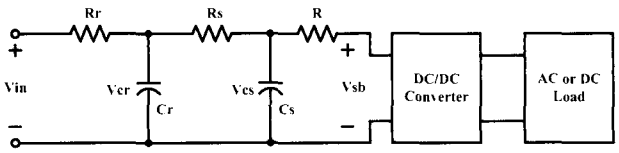

Fig. 4. Equivalent circuit model of a fuel cell power system.

By simulating the above equivalent circuit of Fig. 4, the system operation characteristics can be investigated. In order to achieve a fast system response, the DC/DC or DC/AC converter can utilize its short time-constant for control purposes. However, eventually the fuel has to be controlled despite its long time-delay [5]. The inputs to the chemical model of a fuel cell include mass flows of air (O2) and hydrogen (H2), cooling water, relative humidity of oxygen and hydrogen, and the load resistance. The outputs from the chemical model include temperature of the cell, power loss, internal resistance, heat output, efficiency, voltage, and total power output [6]. Generally, in case of excess of hydrogen supply, it is re-circulated in order to avoid any wastage.

4. Electrical Modeling of Photovoltaic (PV) Cells

As aforementioned, photovoltaic systems have been studied widely as a renewable energy source, because not only they are environmentally friendly, but they also have infinite energy available from the sun. Although the PV systems have the above-mentioned advantages, their study involves precise management of factors such as solar irradiation and surface temperature of the PV cell [7]. The PV cells typically show varying *v-i* characteristics depending on the factors mentioned above. Fig. 5 shows the output characteristics of a PV cell with changing levels of illumination.

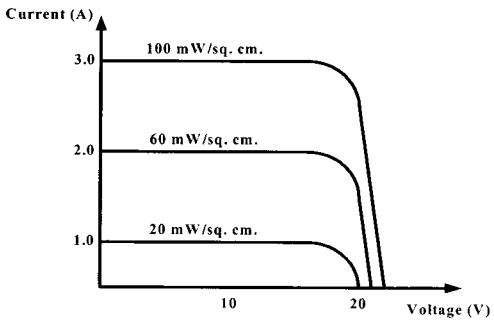

Fig. 5. Typical *v-i* characteristics of a PV cell with varying illumination levels.

As is clear from Fig. 5, the current level increases with the increase in the irradiation level. Fig. 6 shows the *v-i* curves with varying cell temperatures.

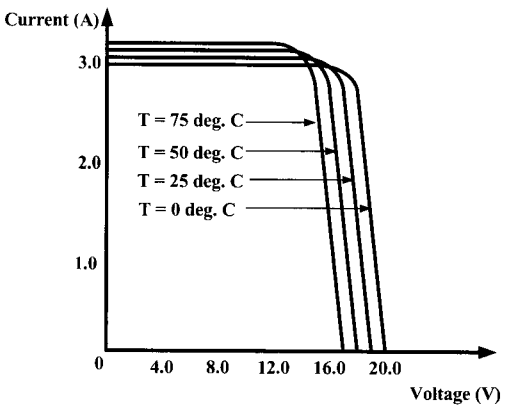

Fig. 6. Typical *v-i* characteristics of a PV cell with varying cell temperatures.

As depicted in Fig. 6, the output curves for varying cell temperatures show higher voltage level as the cell temperature increases. Therefore, while modeling the PV cell, adequate consideration must be given to these two characteristics in particular.

Keeping the above-mentioned factors in mind, the electrical equivalent circuit modeling approach is proposed here. This model is basically a non-linear distributed circuit, in which the circuit elements consist of familiar semiconductor device parameters. Eventually, running a suitable computer simulation can easily simulate this model.

The PV cell can basically be considered as a current source with the output voltage primarily dependent on the load connected to its terminals [8]. The equivalent circuit model of a typical PV cell is as shown in Fig. 7.

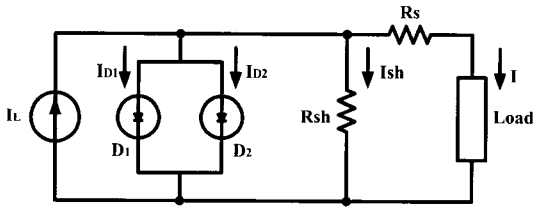

Fig. 7. Schematic of equivalent circuit model of a PV cell.

Suitable forward bias (illuminated) and reverse bias (dark) tests can be performed on the PV cell, in order to generate the *v-i* curves similar to those in Figs. 5 and 6. As is clear from Fig. 7, there are various parameters involved in the modeling of a typical PV cell. These parameters are:

I_L – light generated current (A),

I_{D1} – diode saturation current (A),

I_{D2} – additional current due to diode quality constant (A),

I_{sh} – shunt current (A),

R_s – cell series resistance (Ω),

R_{sh} – cell shunt resistance (Ω), and

I – cell generated current (A).

The model depicted in Fig. 7 examines all the characteristic measurements of the p-n junction cell type. From the above circuit, the following equation for cell current can be obtained:

$$J = J_L - J_{o1}\left\{\exp\left[\frac{q(V+J.R_s)}{kT}\right]-1\right\}- Jon\left\{\exp\left[\frac{q(V+J.R_s)}{A.kT}\right]-1\right\}-G_{sh}(V+J.R_s) \quad (3)$$

Here, q is the electron charge and k is the Boltzman's constant. The voltage at the terminals of the diodes in Fig. 7 can be expressed as follows:

$$V = V_{oc} - IR_s + \frac{1}{\Delta}\log_n\left\{\frac{\beta(I_{sc}-I)-V/R_{sh}}{\beta.I_{sc}-V_{oc}/R_{sh}}+\exp\left[\Delta(I_{sc}.R_s-V_{oc})\right]\right\} \quad (4)$$

Here, β is the voltage change temperature coefficient (V/°C).

For the PV cell model of Fig. 7, *Rs* and *Rsh* are usually estimated when the cell is not illuminated. The series resistance, *Rs*, represents the ohmic losses in the front surface of the PV cell, whereas, the shunt resistance, *Rsh*, represents the loss due to diode leakage currents. Thus, these values can be approximated from the dark characteristic curve of the cell. The generated light current (I_L) is calculated by the collective probability of free electrons and holes. It can be expressed as follows:

$$I_L = q.N[\Sigma f_c(x_N)+\Sigma f_c(x_P)+2l] \quad (5)$$

Here, $f(x)$ is the probability distribution function and N is the rhythm of generated electrons and holes. Once the equations of the cell model are formulated, the efficiency of the PV cell can be obtained as:

$$Efficiency = P_{out}/P_{in} = f.I_{sc}.V_{oc}/P_{in} \quad (6)$$

A distinct advantage of such a computer model is the fact that, with a very few number of changes, it can receive data from different kinds of PV cells maintaining satisfactory results [8]. An example of such a PV model used in conjunction with a power electronic intensive system is shown in Fig. 8.

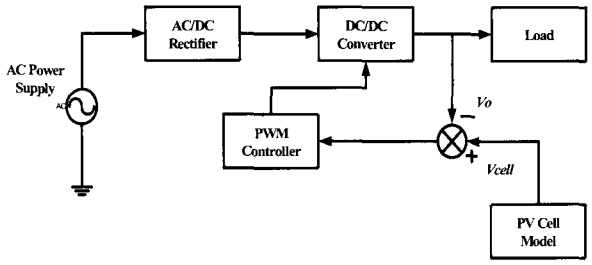

Fig. 8. Schematic of a PV cell model-based system for simulation.

The vital part of the system, as depicted in Fig. 8, is the DC/DC converter. The DC/DC converter could be a boost, buck, or buck-boost converter. Although, in the system shown in Fig. 8, it is valid to assume a buck or buck-boost DC/DC converter, it becomes erroneous to assume usage of a boost converter. This is because the DC/DC boost converter does not make use of the full voltage range.

5. Electrical Modeling of Ultra -capacitors (UC)

Ultra-capacitors (also known as double-layer capacitors) work on the electro-chemical phenomenon of very high capacitance/unit area, and use an interface between electrode and electrolyte [9]. Typical values of such capacitors range from 400 F - 800 F and have low values of resistivity (approximately 10^{-3} Ω-cm) [9], [10]. These UCs operate at high energy densities, which are commonly required for applications such as space communications, digital cellular phones, electric vehicles, and hybrid electric vehicles. In some cases, usage of a hybridized system employing a battery alongside the UC provides an attractive energy storage system, which offers numerous advantages. This is particularly due to the fact that the UC provides the necessary high power density whereas the battery provides the desired high energy

density. Such a hybridized model will be covered here.

5.1 Double Layer UC Model

A simple electrical equivalent circuit of a double layer UC is shown in Fig. 9. Its parameters include equivalent series resistance (ESR), equivalent parallel resistance (EPR), and the overall capacitance. The ESR in Fig. 9 is important during charging/discharging since it is a lossy parameter, which, in turn, causes the capacitor to heat up. On the other hand, the EPR has a leakage effect and, hence, it only affects the long-term storage performance [9].

For the purpose of simplification in calculations, the EPR parameter is dropped.

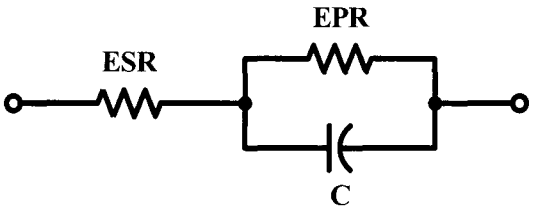

Fig. 9. Electrical equivalent circuit of an ultra-capacitor.

Furthermore, the dropping of the EPR parameter does not have any significant impact on the results. The circuit for analysis is thus simply an ideal capacitor in series with a resistance and the corresponding load [9]. Hence, the value of resistance can be written as:

$$R = n_s \frac{ESR}{n_p} \tag{7}$$

Here, R is the overall resistance (Ω), n_s is the number of series capacitors in each string and n_p is the number of parallel strings of capacitors. Furthermore, the value for the total capacitance can be expressed as:

$$C = n_p \frac{C_{rated}}{n_s} \tag{8}$$

Here, C is the overall value of capacitance and C_{rated} is the capacitance of individual capacitor. This model can be used in conjunction with a DC/DC converter, which, in turn, acts as a constant power load, as shown in Fig. 10.

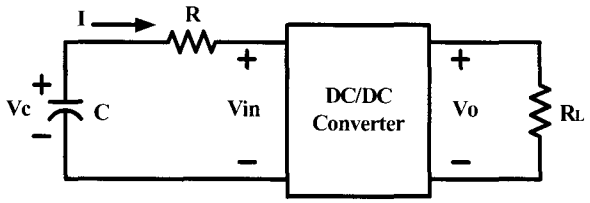

Fig. 10. Circuit showing UC connected to a constant power load.

The capacitor bank can be used in stand-alone mode or can be operated in parallel with a battery of suitable size for the applications mentioned earlier. A brief description of such a hybrid model is described in the following section.

5.2 Battery/UC Hybrid Model

As stated earlier, combining a battery and an UC to operate in parallel makes an attractive energy storage system with many advantages. Such a hybrid systems uses both the high power density of the UC as well as the high energy density of the battery. In this section, an electrical equivalent model of such a system will be presented, which can be used to evaluate its voltage behavior. The model is as depicted in Fig. 11.

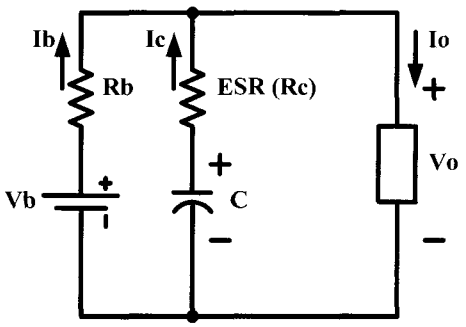

Fig. 11. Equivalent circuit model of a battery/UC hybrid system.

The equivalent circuit of Fig. 11 shows an equivalent series resistance (*Rc*) and a capacitor (*C*) as a model of the UC whereas the Li-ion battery can be modeled simply by using a series resistance (*Rb*) and a battery. The values of *Rc* and *C* depend on the frequency due to the porous nature of the electrodes of the UC [10]. When the pulse-width (T) is varied, the discharge rate of the UC can be varied and can be shown to be equal to a frequency of

$f = 1/T$. The following equations can be written for Io and Vo from the equivalent circuit model of Fig. 10:

$$I_o = I_c + I_b \tag{9}$$

$$V_o = V_b - I_b R_b = \left[V_b - \frac{1}{C} \int_0^T I_c . dt \right] - I_c R_c \tag{10}$$

Here, I_o and V_o are the output current and voltage delivered to the load respectively. From the above two equations, it is possible to achieve a voltage drop $\Delta V = V_b - V_o$ due to a pulse current of I_o. This voltage drop can be finally expressed as:

$$\Delta V = \frac{I_o R_b R_c}{R_b + R_c + \frac{T}{C}} + \frac{I_o R_b \frac{T}{C}}{R_b + R_c + \frac{T}{C}} \tag{11}$$

The currents delivered by the battery (I_b) and capacitor (I_c) can also be derived and their ratio can be expressed as:

$$\frac{I_c}{I_b} = \frac{R_b}{R_c + \frac{T}{C}} \tag{12}$$

It can be seen that for a long pulse I_c can be limited by the value of C. Furthermore, it can be concluded that during the pulsed discharge, about 40-50% of the total current is delivered by C. Upon computer simulation of the equivalent circuit model, it is possible to study the fact that, during peak power demand, UC delivers energy to assist the battery whereas, during low power demand, UC receives energy from the battery [10].

Due to the advanced energy storage capabilities of the UC, it can be used for applications requiring repeated short bursts of power such as in vehicular propulsion systems. In a typical scenario, both the battery and the UC provide power to the motor and power electronic DC/AC inverter during acceleration and overtaking whereas they receive power via regenerative braking during slow down/deceleration [11]. Two most popular topologies for inserting batteries and UCs into drivetrains are as shown in Figs. 12(a) and 12(b).

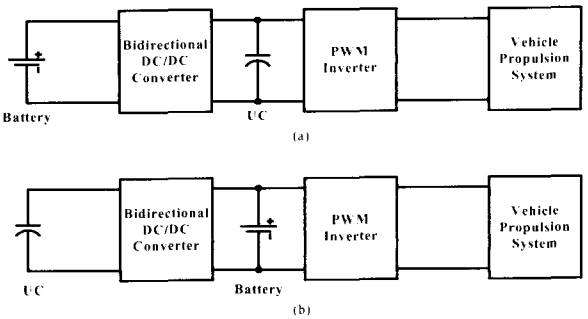

Fig. 12. Typical topologies of batteries and UCs in drivetrains.

As is clear in the topology of Fig. 12(a), the UC bank is placed on the DC bus whereas in Fig. 12(b), the DC bus houses the battery. Amongst the two topologies, the one of Fig. 12(a) has a much more degraded energy efficiency since the whole of the battery energy has to go through the DC/DC converter. Another drawback worth highlighting is that a very high voltage UC bank is required, which is extremely expensive. Hence, more often than not, the topology of Fig. 12(b) is generally considered for HEV applications [11]. In a typical brushless DC (BLDC) motor driven electric vehicle propulsion system, an UC bank could be used to achieve a wider drive range, good acceleration/deceleration performance, and to lower the costs.

Future projections with regards performance of UCs show that energy densities of as high as 10-20 Wh/kg are easily achievable using carbon electrode materials with specific capacitance values of nearly 150-200 F/gm [12].

Currently, extensive R&D on UCs is being carried out in the US, Canada, Europe, and Japan. As aforementioned, most of the research on UCs focuses on EV and HEV applications as well as medical and power system applications.

6. Electrical Modeling of Flywheel Energy Storage Systems (FESS)

Flywheels are most definitely finding numerous applications as energy storage devices in various power system configurations. Furthermore, the constant improvement in digital signal processing (DSP) and microprocessor technologies in conjunction with the recent development in magnetic material technology makes this fact a distinct possibility. A flywheel energy storage system (FESS) is advantageous in a system

comprising of other secondary storage devices such as batteries since it is capable of generating optimum charge/discharge profiles for specific battery charac -teristics [13]. This fact facilitates the exploration of the benefits for optimizing battery management.

A rotating flywheel can store mechanical energy in the form of kinetic energy based on its inertial properties. Essentially, a FESS consists of a rotor, a motor/generator system, and a suitable enclosure [14]. An example of a flywheel energy storage system used as a voltage regulator as well as UPS system is as shown in Fig. 13.

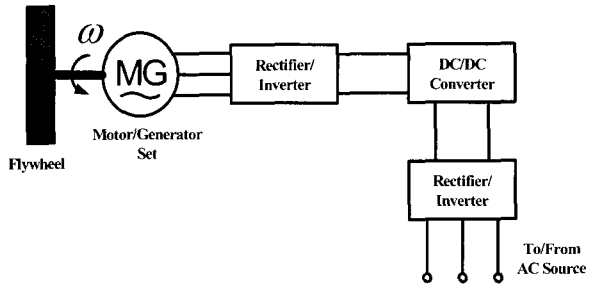

Fig. 13. Typical FESS employed as voltage regulator and UPS.

The system of Fig. 13 essentially operates in 3 modes, namely charging mode, voltage regulation mode, and UPS mode [15]. The motor/generator (M/G) set, as shown in Fig. 13, is required for energy storage purposes in the form of the inertia of the rotor. At some suitable point in the operation of the system, it retrieves this stored energy as demanded by the load. The M/G set is a high-speed device, which basically operates in the motoring mode when charging the flywheel and in the generating mode when discharging it. The motor used for the M/G set could be a brushless DC motor of appropriate rating. The FESS can be easily simulated using the following equation:

$$V_x = R \times i_x + (L - M)\frac{di_x}{dt} + E_x \tag{13}$$

Here, V_x, i_x, and E_x are the voltages, stator currents, and back-EMFs for the 3 phases of the BLDC motor, respectively. In addition, R, L, and M are the resistance, self-inductance, and mutual inductance of the stator winding [16]. The back-EMF is directly proportional to the mechanical speed, ω_m, and the rotor angle, θ_r.

In order to electrically simulate the same flywheel energy storage system operating in conjunction with power electronic intensive systems, it is essential to derive an equivalent electrical model of the same. For this purpose, it is critical to note the important mathematical equations that describe the above system. These are as shown below:

$$v = R.i + L\frac{di}{dt} + a\omega \tag{14}$$

$$T_{em} = a.i = J_r\frac{d\omega}{dt} + b\omega + T_L \tag{15}$$

$$T_L = J\frac{d\omega}{dt} \tag{16}$$

Here, v is the voltage across the motor terminals; i is the electric current through the motor; ω is the rotor speed; T_{em} is the electromagnetic torque imposed on the rotor; T_L is the mechanical torque imposed on the rotor by the flywheel; J_r is the equivalent moment of inertia of the rotor; J is the moment of inertia of the flywheel; and, R and L are the armature resistance and self-inductance. Furthermore, a indicates the ratio of the rated voltage of the motor to its rated speed whereas b indicates the mechanical drag coefficient [17]. The electrical equivalent circuit generated by combining the above 3 equations is depicted in Fig. 14.

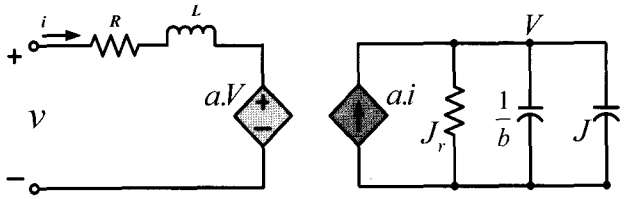

Fig. 14. Electrical equivalent circuit of a flywheel energy storage system.

It is essential to note that the circuit parameters used are basically the parameters employed for the definition of the mathematical model of the FESS. Thus, Fig. 14 describes the FESS system in its entirety via an electrical equivalent. Again, as aforementioned, the task of simulating a FESS with any electrical system becomes immensely simplified since such an electrical model can be constructed in any popular electrical CAD simulation software and can be appropriately analyzed.

7. Conclusions

This paper has essentially dealt with the electrical modeling techniques of major types of renewable energy sources and efficient energy storage devices, namely batteries, fuel cells, PV cells, ultra-capacitors, and flywheels. These models can easily be simulated and validated for their performance by running a simple computer simulation. In addition, presented in this paper are the various applications where these popular renewable energy sources and storage devices are employed, thus, making their modeling and simulation studies worthwhile.

References

[1] Y-H. Kim and H-D. Ha, "Design of Interface Circuits with Electrical Battery Models," *IEEE Trans. on Industrial Electronics*, Vol. 44, No. 1, pp. 81-86, Feb. 1997.

[2] H. L. Chan and D. Sutanto, "A New Battery Model for use with Battery Energy Storage Systems and Electric Vehicles Power Systems," in Proc. IEEE Power Engineering Society Winter Meeting, Singapore, No. 1.1, pp. 470-475, Jan. 2000.

[3] J. Marcos, A. Lago, C. M. Penalver, J. Doval, A. Nogueira, C. Castro, and J. Chamadoira, "An Approach to Real Behavior Modeling for Traction Lead-Acid Batteries," in Proc. IEEE 32nd Annual Power Electronic Specialists Conf., Vancouver, BC, Canada, Vol. 2, pp. 620-624, June. 2001.

[4] H-G. Jeong, B-M. Jung, S-B. Han, S. Park, and S-H. Choi, "Modeling and Performance Simulation of Power Systems in Fuel Cell Vehicles," in Proc. 3rd International Power Electronics and Motion Control Conf., Beijing, China, Vol. 2, pp. 671-675, Aug. 2000.

[5] Y-H. Kim and S-S. Kim, "An Electrical Modeling and Fuzzy Logic Control of a Fuel Cell Generation system," IEEE Trans. on Energy Conversion, Vol. 14, No. 2, pp. 239-244, Jun. 1999.

[6] W. Turner, M. Parten, D. Vines, J. Jones, and T. Maxwell, "Modeling of a PEM Fuel Cell for Use in a Hybrid Electric Vehicle," in Proc. 49th IEEE Vehicular Technology Conf., Amsterdam, The Netherlands, Vol. 2, pp. 1385-1388, Sept. 1999.

[7] J-H. Yoo, J-S. Gho, and G-H. Choe, "Analysis and Control of PWM Converter with V-I Output Characteristics of Solar Cell," in Proc. *2001 IEEE International Symposium on Industrial Electronics*, Pusan, Korea, Vol. 2, pp. 1049-1054, Jun. 2001.

[8] G. A. Vokas, A. V. Machias, and J. L. Souflis, "Computer Modeling and Parameters Estimation for Solar Cells," in Proc. 6th Mediterranean Electrotechnical Conf., Ljubljana, Slovenia, Vol. 1, pp. 206-209. May. 1991.

[9] R. L. Spyker and R. M. Nelms, "Double Layer Capacitor/DC-DC Converter System Applied to Constant Power Loads," in Proc. IEEE 31st Intersociety Energy Conversion Engineering Conf., Washington, DC, Vol. 1, pp. 255-259, Aug. 1996.

[10] J. P. Zheng, T. R. Jow, and M. S. Ding, "Hybrid Power Sources for Pulsed Current Applications," *IEEE Trans. on Aerospace and Electronic Systems*, Vol. 37, No. 1, pp. 288-292, Jan. 2001.

[11] X. Yan and D. Patterson, "Improvement of Drive Range, Acceleration, and Deceleration Performance in an Electric Vehicle Propulsion System," in Proc. IEEE 30th Annual Power Electronic Specialists Conf., Charleston, South Carolina, Vol. 2, pp. 638-643, June. 1999.

[12] A. F. Burke, "Prospects for Ultracapacitors in Electric and Hybrid Vehicles," in Proc. IEEE 11th Annual Battery Conf. on Applications and Advances, Long Beach, CA, pp. 183-188, Jan. 1996.

[13] B. G. Beaman and G. M. Rao, "Hybrid Battery and Flywheel Energy Storage System for LEO Spacecraft," in Proc. IEEE 13th Annual Battery Conf. on Applications and Advances, Long Beach, CA, pp. 113-116, Jan. 1998.

[14] L. J. Reinke, "Tutorial Overview of Flywheel Energy Storage in a Photovoltaic Power Generation System," in Proc. *IEEE Canadian Conf. on Electrical and Computer Engineering*, Vancouver, Canada, Vol. 2, pp. 1161- 1164. Sept. 1993.

[15] R. S. Weissbach, G. G. Karady, and R. G. Farmer, "A Combined Uninterruptible Power Supply and Dynamic Voltage Compensator using a Flywheel Energy Storage System," *IEEE Trans. on Power Delivery*, Vol. 16, No. 2, Apr. 2001.

[16] T. Boutot, L. Chang, and D. Luke, "A Low Speed Flywheel System for Wind Energy Conversion," in Proc. *IEEE Canadian Conf. on Electrical and Computer Engineering*, Winnipeg, Vol. 1, pp. 251-256, Canada, May. 2002.

[17] Z. Jiang, "Flywheel Energy System Virtual Test Bed (VTB) Model," see http://vtb.engr.sc.edu/.

Sheldon S. Williamson received his B.S. degree in Electrical Engineering from Bombay University, India in 1999. He received his M.S. degree in Electrical Engineering specializing in power electro nics and motor drives in 2002 from the Illinois Institute of Technology, Chicago, USA. He is currently

pursuing his Ph.D. degree in Electrical Engineering at the Illinois Institute of Technology under the guidance of Prof. Emadi. His research deals with Advanced Drive Train Configurations for Hybrid Electric Vehicles.

S. Chowdary Rimmalapudi was born in Andhrapradesh, India, in 1979. He received the B.S. degree in electrical engineering from Regional Engineering College (REC), Rourkela, in 2001, and the M.S. degree in electrical and computer engineering from the Illinois Institute of Technology, Chicago, in 2003. Since then, he has been with Aviation Instrument Technologies Inc., Tampa, FL, where he is currently working on research, design, and development of advanced power electronics for aviation. His research interests are in the areas of power electronics and control systems. Mr. Rimmalapudi is a member of IEEE.

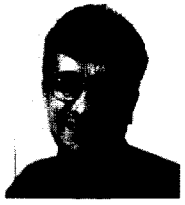

Ali Emadi received the B.S. and M.S. degrees in electrical engineering with highest distinction from Sharif University of Technology, Tehran, Iran. He also received his Ph.D. degree in electrical engineering from Texas A&M University, College Station, TX. He joined the Electrical and Computer Engineering (ECE) Department of Illinois Institute of Technology (IIT) in August 2000. Dr. Emadi is the director of Grainger Power Electronics and Motor Drives Laboratories at IIT where he has established research and teaching laboratories as well as courses in power electronics, motor drives, and vehicular power systems. He is also the co-founder and co-director of IIT Consortium on Advanced Automotive Systems (ICAAS). Dr. Emadi has been named the Eta Kappa Nu Outstanding Young Electrical Engineer for 2003. He is the recipient of the 2002 University Excellence in Teaching Award from IIT as well as Overall Excellence in Research Award from Office of the President, IIT, for mentoring undergraduate students. He directed a team of students to design and build a novel low-cost brushless DC motor drive for residential applications, which won the First Place Overall Award of the 2003 IEEE/DOE/DOD International Future Energy Challenge for Motor Competition. He is an Associate Editor of IEEE Transactions on Power Electronics and a member of the editorial board of the Journal of Electric Power Components and Systems. Dr. Emadi is the author of over 100 journal and conference papers as well as three books including Vehicular Electric Power Systems: Land, Sea, Air, and Space Vehicles, Marcel Dekker, 2003, Energy Efficient Electric Motors: Selection and Applications, Marcel Dekker, 2004, and Uninterruptible Power Supplies and Active Filters, CRC Press, 2004. Dr. Emadi is also the editor of the Handbook of Automotive Power Electronics and Motor Drives, Marcel Dekker, 2005. He is a senior member of IEEE and a member of SAE. He is also listed in the International Who's Who of Professionals and Who's Who in Engineering Academia.